Bioorganic & Medicinal Chemistry Letters 24 (2014) 5478–5483

Contents lists available at ScienceDirect

Bioorganic & Medicinal Chemistry Letters

journal homepage: www.elsevier.com/locate/bmcl

Novel tricyclic pyrazolopyrimidines as potent and selective GPR119 agonists

Mihai Azimioara *, Phil Alper, Christopher Cow, Daniel Mutnick, Victor Nikulin, Gerald Lelais, John Mecom, Matthew McNeill, Pierre-Yves Michellys, Zhiliang Wang, Esther Reding, Michael Paliotti, Jing Li, Dingjiu Bao, Jocelyn Zoll, Young Kim, Matthew Zimmerman, Todd Groessl, Tove Tuntland, Sean B. Joseph, Peter McNamara, H. Martin Seidel, Robert Epple *

Genomics Institute of the Novartis Research Foundation, 10675 John Jay Hopkins Drive, San Diego, CA 92121, United States

ARTICLE INFO

Article history:
Received 23 July 2014
Revised 29 September 2014
Accepted 2 October 2014
Available online 13 October 2014

Keywords:
GPCR agonists
GPR119
Tricyclic pyrazolopyrimidines
Type 2 diabetes

ABSTRACT

Systematic SAR optimization of the GPR119 agonist lead **1**, derived from an internal HTS campaign, led to compound **29**. Compound **29** displays significantly improved in vitro activity and oral exposure, leading to GLP1 elevation in acutely dosed mice and reduced glucose excursion in an OGTT study in rats at doses $\geqslant$10 mg/kg.

Increasing glucose-dependent insulin secretion from the pancreas is a hallmark for the treatment of type 2 diabetes patients. Upon ingestion of long-chain monosaturated fatty acids (MSFAs) present in diets containing carbohydrates and fat, insulin secretion is triggered via several distinct mechanisms: For example, insulin release may be triggered upon binding of MSFAs directly to receptors on pancreatic β cells, such as GPR40,[1] or indirectly upon secretion of incretins (GLP1, GIP, etc.) from enteroendocrine L-cells which in turn act on the appropriate receptors in β cells.[2] The $G\alpha_s$-protein-coupled receptor GPR119 is predominantly expressed in both pancreatic β cells and in enteroendocrine L-cells, stimulating both insulin and incretin secretion in a complementary fashion. GPR119 agonists may therefore provide an exciting and novel approach to the treatment of type-2 diabetes and obesity.[3–6]

As disclosed in our preceding paper,[7] medicinal chemistry SAR optimization of an HTS hit led to the discovery of **1**, a potent and selective GPR119 agonist. This scaffold differs significantly from the 'classical' GPR119 pharmacophore, exemplified by the examples **2**[8] and **3**[9] (Fig. 1).

Notably, compound **1** lacks an essential 'headgroup' (arylsulfone or heterocycle), as well as a piperidine-derived 'tail group'.[10] Compound **1** showed good in vitro activity toward raising cAMP levels via GPR119 human[11] and murine[12] receptors, and demonstrated the ability to secrete GLP-1 and insulin in the respective cell lines. Although it acutely elevated levels of active GLP-1

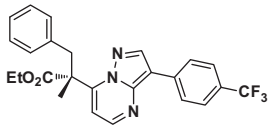

1
hGPR119: 0.007 μM (80%)

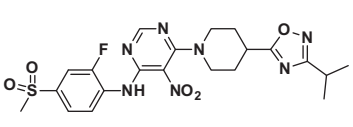

2 (AR231453)
hGPR119: 0.003 μM (100%)

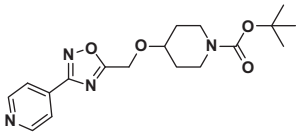

3 (PSN632408)
hGPR119: 0.63 μM (85%)

Figure 1. In-house GPR119 agonist lead **1**, and competitor GPR agonists **2** and **3**.

* Corresponding authors. Tel.: +1 858 332 4606; fax: +1 858 812 1648 (M.A.); tel.: +1 858 812 1720; fax: +1 858 812 1648 (R.E.).
E-mail addresses: mazimioara@gnf.org (M. Azimioara), repple@gnf.org (R. Epple).

http://dx.doi.org/10.1016/j.bmcl.2014.10.010
0960-894X/

Table 1
SAR of the core pyrazolo[1,5-*a*]pyrimidine substitution The numbers in italics are positional labels

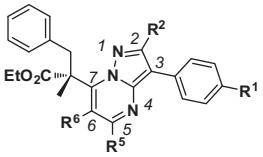

Entry	R^1	R^2	R^5	R^6	hGPR119[a]		mGPR119[a]	
					EC_{50}	Eff (%)	EC_{50}	Eff (%)
4	CF_3	H	H	Me	1	80	11	62
5	Cl	H	Me	H	>10	15		
6	CF_3	Me	H	H	23	83	24	72
7	CF_3	H	H	Cl	3	75	8	73

[a] EC_{50} values in nM; 100% efficacy = max. response of compound **2**.

in vivo inC57Bl/6 mice,[13] it was only marginally active in an acute rat OGTT study.[14] We hypothesized that the low efficacy may be due to three main factors: (1) partial agonism (⩽80%)[11] on the receptor, (2) high plasma protein binding and (3) poor exposure due to low solubility and low metabolic stability. Hence we sought to improve the physicochemical properties of the scaffold while also enhancing its agonistic efficacy on the receptor.

First we expanded the existing SAR of **1** by substituting positions of the pyrrolopyrimidine core not previously investigated. The results depicted in Table 1 suggest that substitution is tolerated in positions 2 and 6 (entries **6**, **4** and **7**, respectively), but not in position 5 (entry **5**). It is noteworthy that in both positions only small substituents such as methyl and halogen groups were tolerated, whereas larger substituents led to loss of GPR119 activity.

However, both potency and efficacy were not improved. We observed a significant drop of activity, especially on the rodent receptor (e.g. compound **4**). Not surprisingly, these compounds did not significantly elevate GLP-1 levels in rodents (data not shown).

In order to gain agonist efficacy on the receptor, we intended to find if there was a preferred 'active' conformation of the scaffold ameliorating the binding and activation of both the human and mouse receptor. One way to sample some of the potential conformations is to reduce the degree of rotational freedom and rigidify the scaffold into a productive, pharmacologically relevant conformation. Hence a number of tricyclic compounds were synthesized, using the 6-position of the scaffold as an anchoring point for cyclizations. The cyclizations involved each of the three substituents of the quaternary carbon next to position 7 of the core (e.g. the ester, methyl or benzyl group), thereby allowing to 'freeze' three distinct conformations of this particular substituent. Cyclizing the ester or the benzylic position with the 6-Me group led to inactive compounds (results not shown), but tying both methyl groups into a ring led to the more restricted analog **8**. Analogs such as **8** consistently

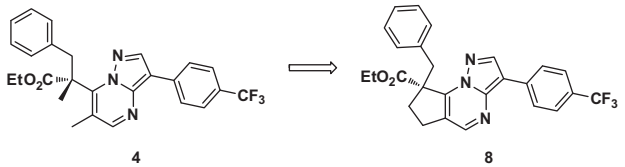

Figure 2. Rigidification of **4** leads to increased GPR119 agonist efficacy.

Table 2
Some selected ADME/PK properties for analogs **1**, **4** and **9**

Entry	*c*log*P*	Precipitation[a]	−log PAMPA	ER[b] (h/r/m)	AUC[c] h*μM
1	5.74	Low	5.5	0.3–0.7	2.1
4	6.19	Med	5.4	0.3–0.5	0.6
8	5.96	High	5.5	0.6–1.0	0.3

[a] Precipitation in PEG/D5W vehicles.
[b] Extraction ratio.
[c] Dose-normalized AUC (po) in Balb/C mice.

displayed high potency with increased agonist efficacy on both human and rodent receptors (Fig. 2).

This increase in receptor activity of compound **8** came at the price of a decrease in exposures compared to the lead compound **1** (Table 2). Whereas *c*log*P* values and permeabilities did not change dramatically, we noticed a further drop in the already poor solubility (generally <5 μM), the extent of which was difficult to pick up in our solubility assay. However, in several organic and aqueous media, there was significantly more precipitation observed for compounds **4** and **8** compared to **1**. The in vitro hepatic clearance (depicted as a range of microsomal extraction ratio in human, mouse and rat liver microsomes) had a clear trend to increase dramatically in the tricyclic system **8**. Concomitantly, oral exposure in mice significantly decreased from **1** to **8** (in vivo hepatic clearance not measured).

We hypothesized that the gains in receptor potency and efficacy for the tricyclic analogs would allow us to implement changes to the scaffold previously not tolerated in the bicyclic series, thereby leading to increased exposures via more favorable physicochemical properties, while keeping activities in the acceptable range required for in vivo efficacy. An SAR summary (human and mouse GPR119 receptor activity, physicochemical properties, metabolic stability) for analogs **8**–**38** is depicted in Table 3.

A general synthetic pathway to these tricyclic structures is described in Scheme 1 (detailed procedures can be accessed in the patent application WO 2011/014520 A2).[15] Benzylation of the appropriate ketoester using KHMDS, followed by treatment with DMF-dimethyl acetal yielded the racemic (dimethylamino)-methylene ketone. The optimal synthetic pathway for enantiomerically pure analogs proved to be analytical resolution (preparative chiral chromatography)[16] at this stage. The final products were afforded by acid-catalyzed condensation with the appropriate 4-aryl aminopyrazole, which was derived from the corresponding aryl acetonitrile via condensation with ethyl formate and subsequent cyclization with hydrazine.

In line with previous observations, the (*R*) enantiomer **8** was significantly more active than the (*S*) enantiomer **9**. The ethyl and methyl esters had similar activities and properties for a variety of analogs (e.g. **8** vs **10**). The 3-fluoro substitution on the benzyl group (R^7 = F in Table 3) did not bring about any major changes (entries **8** vs **11**).

Expansion of the carbocyclic ring beyond the 5-membered carbacycle in **8** led to reduced GPR119 activity (entries **12**–**14**). As described in the preceding report, SAR around the position 3 and 7 of the core heterocycle was rather steep, the more polar substituents being particularly not tolerated. Indeed, small changes in the *para*-substituent of the 3-aryl group led to a marked drop in receptor agonist potency and efficacy (entries **15**–**18**). In an effort to decrease hydrophobicity and increase solubility in the series, we thus focused our attention to the newly formed carbacycle in the tricyclic core. To our surprise, either inserting a heteroatom position 7 of the core heterocycle (entries **19** and **20**) or next to the quaternary carbon (entries **21** and **22**) did not result in a complete loss of GPR119 agonist activity. Even the introduction of a physiological-conditions ionizable secondary amine **22** was well

Table 3
SAR of tricyclic analogs

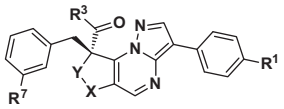

Entry	R^1	R^3	R^7	–X-Y–	hGPR119[a]		mGPR119[a]		*c*log*P*	ER (human)
					EC_{50} (nM)	Eff (%)	EC_{50} (nM)	Eff (%)		
(*R*)-**8**	CF_3	OEt	H	—$(CH_2)_2$—	0.5	85	8	80	5.96	0.96
(*S*)-**9**	CF_3	OEt	H	—$(CH_2)_2$—	38	66	nd	nd	5.96	nd
(±)-**10**	CF_3	OMe	H	—$(CH_2)_2$—	2	82	17	91	5.58	0.93
(*R*)-**11**	CF_3	OMe	F	—$(CH_2)_2$—	3	92	9	81	5.58	0.96
(*R*)-**12**	CF_3	OEt	H	—$(CH_2)_3$—	8	75	27	59	6.52	0.71
(±)-**13**	CF_3	OMe	H	—$(CH_2)_4$—	74	66	nd	nd	6.55	nd
(±)-**14**	CF_3	OEt	H	—$(CH_2)_5$—	101	56	nd	nd	7.64	nd
(*R*)-**15**	Cl	OEt	H	—$(CH_2)_2$—	3	73	11	78	5.79	0.79
(±)-**16**	SO_2Me	OMe	H	—$(CH_2)_2$—	125	81	nd	nd	2.91	0.89
(±)-**17**	CN	OMe	H	—$(CH_2)_2$—	7	55	nd	nd	3.98	nd
(±)-**18**	OPh	OMe	H	—$(CH_2)_2$—	20	60	nd	nd	6.65	nd
(±)-**19**	CF_3	OMe	H	—OCH_2—	11	83	15	76	5.20	0.88
(*R*)-**20**	CF_3	OEt	H	—$NHCH_2$—	25	75	25	80	6.00	0.75
(±)-**21**	CF_3	OMe	H	—CH_2O	34	77	35	78	4.61	0.96
(*S*)-**22**	CF_3	OMe	F	—CH_2NH—	3	91	14	88	4.17	0.95
(±)-**23**	CF_3	OEt	H	—CH_2NMe—	214	55	nd	nd	5.13	nd
(*S*)-**24**	CF_3	OMe	F	—CH=N—	73	84	135	80	3.71	0.97
(±)-**25**	CF_3	OEt	F	—CONH—	298	81	nd	nd	5.02	nd

[a] Assays descriptions are in Refs. 11,12.

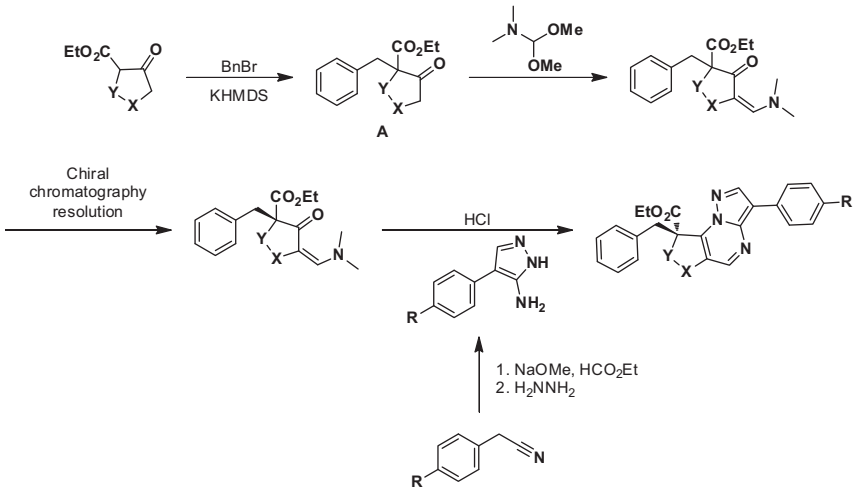

Scheme 1. General approach towards the synthesis of tricyclic pyrazolo[1,5-*a*]pyrimidines. The X and Y substituents are described in Table 3 below.

tolerated, if not beneficial to GPR119 activity. Please note that due to the heteroatom next to the quarternary chiral center, the absolute stereochemical assignment changes from (*R*) to (*S*). Interestingly, methylation to a tertiary amine (entry **23**) was less tolerated. Compound **22** was labile in the presence of human microsomes (ER_h = 0.95), and to a lesser extent in mouse microsomes (ER_m = 0.61). A metabolic ID study revealed that a major metabolite was formed via oxidation of the C—N bond in the 5-membered ring. Hence oxidized analogs **24** and **25** were synthesized and tested for their GPR119 agonist activity. Both compounds had significantly lower activity compared to **22**. Calculated log*P* values indicated a significant 2-log drop going from the carbacycle **8** to the secondary amine **22**. Although there were no precipitation issues observed for these analogs, PK studies in mice showed similarly low oral exposure for amine **22** compared to the carbon analog **8**, indicating that the changes in the 5-membered ring alone were insufficient to positively impact exposures.

Next, we focused our attention on the ester functionality (Table 4). The ester group was seen as a potential liability, although in vitro plasma stability studies did not indicate an inherent instability of the ester group, probably due to steric crowding. Previous investigations deemed the ester essential for GPR119 activity, although a few amide replacements were identified. Transferring these findings to the tricyclic series such as in analog **26** maintained good GPR119 activity and high plasma stability, but solubilities remained low (<5 μM) and extraction ratios remained high (ER_h = 0.9; ER_m = 0.84). Hence, oral exposure in mice did not improve, in fact it was lower (AUC_{dn} = 0.07 μM*h) than for the corresponding ester **22** (AUC_{dn} = 0.31 μM*h). In addition, we found that the tricyclic series also tolerated small alkyl groups in place of the ester functionality (entries **27** and **28**). Specifically, the cyclopropyl analog **28** led to an only 10-fold drop in potency (similar on the rodent receptor), but markedly increased metabolic stability in all species (ER ~ 0.3–0.6).

Table 4
SAR of tricyclic analogs, ester replacement

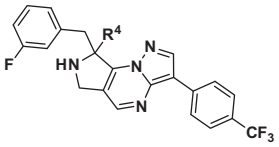

Entry	R^4	hGPR119[a]		ER_h
		EC_{50} (nM)	Eff (%)	
(*S*)-**22**	CO_2Me	3	91	0.95
(*S*)-**26**	$CONMe(CH_2)_2OMe$	2	90	0.90
(±)-**27**	Me	436	77	nd
(±)-**28**	cPr	21	87	0.60

[a] Assays descriptions are in Refs. 11,12.

Compound **28** was synthesized starting from α-cyclopropyl glycine (Scheme 2). After protection of the free amine via methyl carbamate and esterification to the methyl ester, the pyrrolidine core was furnished by condensation with methyl acrylate under basic conditions. Double deprotonation of the pyrrolidine followed by benzylation with the appropriate benzyl halide exclusively on the more nucleophilic carbon gave the fully elaborated quarternary center.[17] Decarboxylation and vinylamine formation gives the cyclization partner for the aminopyrazole, which was accomplished under similar conditions described above. Finally, the methyl carbamate was removed under acidic conditions to afford the desired product.

Up to now we were able to increase receptor agonist efficacy and metabolic stability of the series. Further SAR work was aimed toward improving on the poor solubility profile of the scaffold. We noted that small substituents in position 2 were tolerated (Table 5), and while ionizable groups were deleterious to activity (data not shown), a hydroxymethylene group seemed beneficial for agonist efficacy (entry **29**). For the first time we encountered a compound with measurable solubility (58 μM at pH 6.8) in the series. Moreover, a small polarity change going from a trifluoromethyl-phenyl to a trifluoromethyl-pyridyl substituent in position 3 was also tolerated. Both findings combined (entry **30**) led to a further improvement of the scaffolds physicochemical properties and further improved the solubility of the compound. Unfortunately, we saw a 10 fold decrease in functional potency in an in vitro GLP1 secretion assay using GLUTag cells. As expected, the hydroxymethylene group also posed a considerable metabolic liability, which is reflected in the high ERs of these analogs. Blocking of the metabolic softspot with compounds such as **31** reduced extraction ratio values, but also GPR119 activity. An attempt to slow down metabolism via deuteration of the benzylic position (entries **32** and **33**) or replacement with a primary amide (entry **34**) failed to show the desired impact on extraction ratios and exposures. Replacement of the carboxylate with a cyclopropyl group as described above did not favorably affect metabolic stability either in this case (entries **35** and **36**), and introduced additional Cyp inhibition and induction issues.

Based on the overall acceptable profile, we elected compound **29** to assess its ability to elevate GLP1 in mice acutely in vivo, as well as test its effects on glucose excursion in a 7 day OGTT study in rats (Fig. 3A). After a onetime 10 mg/kg dose, we observed a significant increase of active GLP1 by 29% in mice.[13] After two weeks of once-a-day dosing in ZDF fa/fa rats, we also saw a clear trend in glucose reduction (up to 37% at the 30 mg/kg dose level) following a glucose bolus (Fig. 3B for glucose time course, Fig. 3C for glucose AUC).[15]

In conclusion, we set out to optimize compound **1**, a partial GPR119 agonist that does not fall into the usual GPR119 pharmacophore. Rigidification to a tricyclic system yielded potent full agonists, albeit with a further deterioration of the scaffolds poor physicochemical properties and metabolic stabilities. However, the increased potency level allowed us to implement several changes addressing both poor solubility and metabolic stability while staying in the acceptable activity range on the receptor. We learned that walking into the hydrophobic trap may not always have to be avoided at all costs, but sometimes it can open doors to previously-unacceptable derivatizations in the scaffold. We achieved a remarkable >4 log unit drop in *c*log*P* values going from analog **8** to analog **30** without loss of efficacy on the receptor, leading to measurable solubility in the series. Unfortunately, the most potent compounds with the highest solubilities did not show markedly improved metabolic stabilities and were only moderately exposed in rodents. Nevertheless, in addition to robust GLP1 elevation in mice we also observed a clear trend in glucose reduction in a 2 week OGTT model in rats, rendering this series a rare GPR119 agonist scaffold outside the typical GPR119 pharmacophore displaying the desired in vivo effects in rodents.

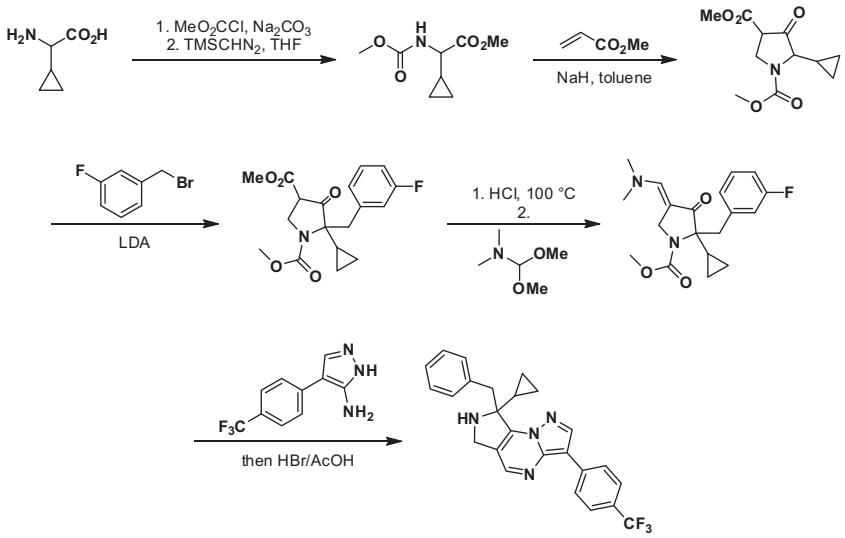

Scheme 2. Synthesis of compound **28**.

Table 5
Additional SAR for positions R^2 and R^4 leading to soluble analogs

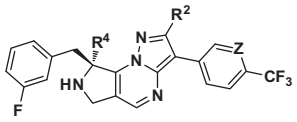

Entry	R^2	R^4	Z	hGPR119[a]		*c*log*P*	Sol (μM)	ER human	GLP1 secretion	AUC (m, 20) (μM*h)
				EC_{50} (nM)	Eff (%)					
29	CH_2OH	CO_2Me	CH	5	99	2.83	58	0.82	0.04	7.65
30	CH_2OH	CO_2Me	N	15	101	1.48	99	0.82	0.65	nd
31	CMe_2OH	CO_2Me	CH	530	58	5.20	nd	0.51	nd	nd
32	CD_2OH	CO_2Me	CH	2	103	2.83	26	0.83	0.09	7.89
33	CD_2OH	CO_2Me	N	35	87	1.48	83	0.85	0.44	6.56
34	$CONH_2$	CO_2Me	CH	20	74	2.59	39	0.92	0.06	nd
35	CH_2OH	cPr	CH	2	88	3.91	6	0.90	0.03	nd
36	CH_2OH	cPr	N	6	82	2.57	36	0.93	0.12	nd

[a] Assays descriptions are in Refs. 11,12.

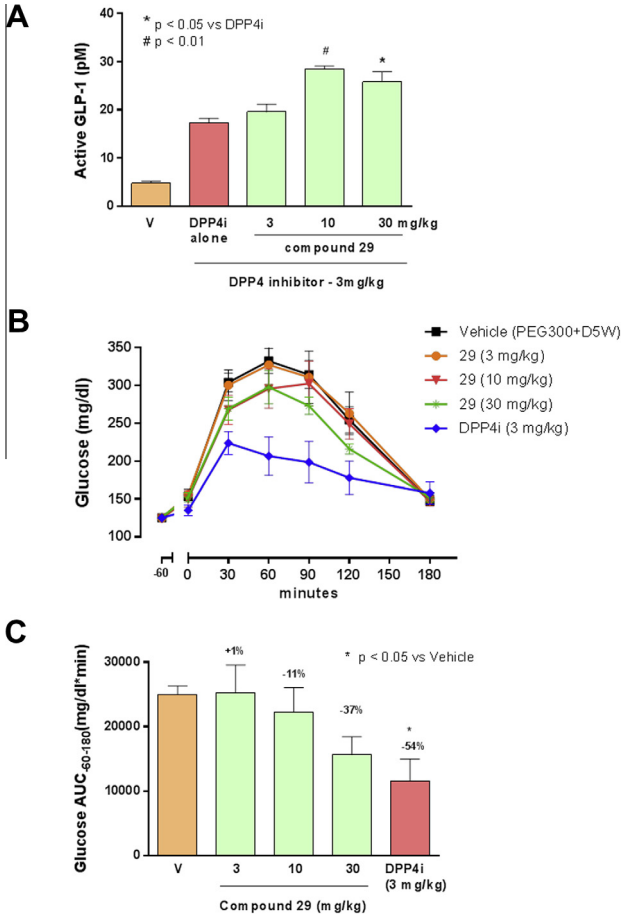

Figure 3. C57BL/6 mouse GLP1 (A) and Zucker fa/fa rat OGTT (B, C) study results for **29**. See footnote 13 (GLP-1) and 14 (OGTT) for study descriptions.

Supplementary data

Supplementary data (crystallographic data and detailed synthetic procedures) associated with this article can be found, in the online version, at http://dx.doi.org/10.1016/j.bmcl.2014.10.010.

References and notes

1. Ichimura, A.; Hirasawa, A.; Hara, T.; Tsujimoto, G. *Prostaglandins Other Lipid Mediat.* **2009**, *89*, 82; Itoh, Y. et al *Nature* **2003**, *422*, 173; Mancini, A. D.; Poitouts, V. *Trends Endocrinol. Metabol.* **2013**, *24*, 398.
2. Drucker, D. J.; Nauck, M. A. *Lancet* **2006**, *368*, 1696.
3. Overton, H. A.; Fyfe, M. C.; Reynet, C. *Br. J. Pharmacol.* **2008**, *153*, S76.
4. Lan, H.; Lin, H. V.; Wang, C. F.; Wright, M. J.; Xu, S.; Kang, L.; Juhl, K.; Hedrick, J. A.; Kowalski, T. J. *Br. J. Pharmacol.* **2012**, *165*, 2799.
5. Hansen, H. S.; Rosenkilde, M. M.; Holst, J. J.; Schwartz, T. W. *Trends Pharmacol. Sci.* **2012**, *33*, 374.
6. Ohishi, T.; Shigeru, Y. *Expert Opin. Invest. Drugs* **2012**, *21*, 321.
7. Alper, P.; Azimioara, M.; Cow, C.; Mutnick, D.; Nikulin, V.; Michellys, P.-Y.; Wang, Z.; Reding, E.; Paliotti, M.; Li, J.; Bao, D.; Zoll, J.; Kim, Y.; Zimmerman, M.; Groessel, T.; Tuntland, T.; Joseph, S. B.; McNamara, P.; Seidel, H. M.; Epple, R. *Bioorg. Med Chem. Lett.* **2014**, *24*, 2383.
8. Semple, G. F.; Fioravanti, B.; Pereira, G.; Calderon, I.; Uy, J.; Choi, K.; Xiong, Y.; Ren, A.; Morgan, M.; Dave, D.; Thomsen, W.; Unett, D. J.; Xing, C.; Bossie, S.; Carroll, C.; Chu, Z.-L.; Grottick, A. J.; Hauser, E. K.; Leonard, J.; Jones, R. M. *J. Med. Chem.* **2008**, *51*, 5172.
9. Overton, H. A.; Babbs, A. J.; Doel, S. M.; Fyfe, M. C. T.; Gardner, L. S.; Griffin, G.; Jackson, H. C.; Procter, M. J.; Rasamison, C. M.; Tang-Christensen, M.; Widdowson, P. S.; Williams, G. M.; Reynet, C. *Cell Metab.* **2006**, *3*, 167.
10. Zhu, X.; Zhu, X.; Huang, D.; Lan, X.; Tang, C.; Zhu, Y.; Han, J.; Huang, W.; Qian, H. *Eur. J. Med. Chem.* **2011**, *46*, 2901.
11. The GPR119 agonist activity of the compounds is tested in a CHO stable cell line overexpressing human GPR119 (Lonza). The compound-induced activation of GPR119 leads to an increase of cellular cAMP production, which is measured with a cAMP HTRF kit (Cisbio). The efficacy of the receptor activation is normalized to AR231453 (compound **2**) being 100%.
12. The compound activity on human or mouse GPR119 is measured with a cAMP HTRF assay in CHO cells overexpressing hGPR119 or mGPR119. Compound-induced GLP-1 secretion is measured in a mouse enteroendocrine cell line GLUTag. The secreted GLP-1 in the supernatant of cells treated with GPR119 agonist is detected with a HEK293 reporter cell line that co-expresses GLP-1 receptor and CRE-luciferase constructs. GPR119 agonist-induced insulin secretion in a hamster beta cell line HIT-T15 is measured with an insulin HTRF kit from Cisbio. The efficacy of the compounds in these assays is normalized to AR231453 (compound **2**) being 100%. Compounds of interest with activities of <100 nM in the human GPR119 were submitted for selectivity testing against a panel of GPCRs; no activities <2 μM were observed for any of the compounds tested in this panel, except for the murine and rat GPR119 assays.
13. Groups of wild-type C57BL/6 J mice ($n = 8$ mice per group) were randomized into treatment groups based on their initial body weight. Mice were housed four per cage and orally dosed with vehicle (v), DPP-4 inhibitor alone, or DPP-4 inhibitor and compound **29**, in a single dose. A glucose bolus (3 g/kg) was delivered thirty minutes post dosing. Sample was collected 2 minutes post glucose bolus. All animals were fasted for 16 hours prior to compound administration. Blood was obtained via retro-orbital bleeding to measure plasma levels of active GLP-1. Approximately 200 μL samples of blood were removed for analysis at 62 min post dosing (2 min post glucose bolus). Active GLP-1 was measured using Glucagon-like peptide-1 (active) ELISA Kit, 96-well plate (Linco Research, Inc.). All procedures in this study were approved by the GNF animal care and use committee and were in compliance with the Animal Welfare Act Regulations 9 CFR Parts 1, 2 and 3, and US regulations (Guide for the Care and Use of Laboratory Animals, 1995).

14. Groups of 9-week old Zucker fa/fa rats (from Charles River) ($n = 6$ rats per group) were randomized into treatment groups based on their initial body weight. Two rats were housed per cage and orally dosed with vehicle (v), DPP-4 inhibitor (DPP4i), or compound **29**, in a single dose. All animals were fasted for 16 h prior to compound administration. A glucose bolus (3 g/kg) was delivered one hour post dosing. Blood was obtained via nipping tail at indicated time points to measure glucose. Glucose AUC was calculated from time −60 min to 180 min. All procedures in this study were approved by the GNF animal care and use committee and were in compliance with the Animal Welfare Act Regulations 9 CFR Parts 1, 2 and 3, and US regulations (Guide for the Care and Use of Laboratory Animals, 1995).
15. Alper, P.; Azimioara, M.; Cow, C.; Epple, R.; Lelais, G.; Mutnick, D.; Nikulin, V. Compounds and compositions as modulators of GPR119 activity, International patent application WO 2011/014520 A2. The absolute chirality was determined by starting with the chiral benzyl ketoester [for example, in Scheme 1, compound **A** with $X = Y = CH_2$, the (*R*) enantiomer is (−) levorotatory; see Deng, Q. -H.; Wadepohl, H; Gade, L. H., *J. Am. Chem. Soc.* **2012**, 134, 2946 and references therein].
16. Example of typical chiral separation conditions (X = H and Y = Me): 21 × 250 mm ChiralPak IC column, 80:20 CO_2/MeOH, 80 g/min, 175 bar, 40 °C, 10 min run time. The desired enantiomer has $t_r = 5.41$ min, the undesired one has $t_r = 4.21$ min. More examples are presented in the Supplementary material.
17. For an example, see International patent WO 2006/005551.